Digital Filtering of Electric Thruster Time Domain Radiated Emissions

IEPC-2019-A242

Presented at the 36th International Electric Propulsion Conference
University of Vienna, Austria
September 15-20, 2019

Nicolas A. Rongione*, William G. Tighe†, Matthew S. Feldman‡, Rostislav Spektor§

and

Michael S. Yonezaki¶
The Aerospace Corporation, El Segundo, CA, 90245, United States of America

Advances in computing have made post-processing of time domain radiated emissions readily accessible. We have previously demonstrated the ability to use a single 400 μs oscilloscope trace with very high sampling rate (20 GS/sec) to resolve the frequency content of electromagnetic radiated emissions in a representative electric propulsion device, Aerospace's GPT-1 Hall thruster. In this paper digital filters have been developed that enable us to sift through the frequency and time domains to be able to 1) build a narrowband time domain trace, 2) monitor the peak amplitude radiated emissions over time in a band ("zero span"), 3) build bit error rate statistical analysis on the data, and 4) recover frequency information over time using the Short-Time Fourier Transform with sufficient overlap. Given the non-stationary nature of electric thruster plasma plumes and intermittent, non-stationary pulsed behavior, often present in Hall thrusters, this study has motivated ongoing investigations into using wavelets that will seek to ensure that peak transient amplitudes are indeed being captured and observe the presence or absence of frequency hopping behavior.

Nomenclature

$DFFT$	= Discrete Fast Fourier Transform
$I - DFT^{-1}$	= Inverse Discrete Fourier Transform
$STFT$	= Short-Time Fourier Transform
Δf	= Frequency Resolution
CWT	= Continuous Wavelet Transform
FFT	= Fast Fourier Transform
POI	= Probability of Intercept
BER	= Bit Error Rate
$RTSA$	= Real-Time Spectrum Analysis

*Propulsion Technical Engineering Staff, Electric Propulsion & Plasma Science, nicolas.a.rongione@aero.org.
†Research Scientist, Electric Propulsion & Plasma Science, william.g.tighe@aero.org.
‡Research Scientist, Electric Propulsion & Plasma Science, matthew.s.feldman@aero.org.
§Laboratory Manager, Electric Propulsion & Plasma Science, rostislav.spektor@aero.org.
¶Engineering Specialist, Antenna Systems, michael.s.yonezaki@aero.org.

I. Introduction

Higher satellite operating powers and an increase in the number of satellites using electric propulsion devices elevate the risk of electromagnetic interference in the form of coherent pulsed emissions that can disrupt satellite communications in an increasingly congested space environment. In fact, the effect of operating an electric propulsion device on orbit has been measured to have a manageable, but measurable influence on communication systems, in at least one case.[1] Traditionally, time domain radiated emissions are utilized to improve the Probability Of Intercept (POI), characterize and capture the spectral content of coherent emissions, and generate a corresponding statistical distribution for determination of a Bit-Error Rate (BER) impact on communication systems.[2] In general, broadband and narrowband data acquisition is taken using an oscilloscope and spectrum analyzer, respectively. The measurement configuration for the spectrum analyzer is taken to model a typical satellite transceiver consisting of an antenna signal fed through an analog, electronic filter. However, since the spectrum analyzer and electronic filter combination is band-limited, it is costly and time consuming to discern the emission levels across the frequency domain. Radiated emissions historically have been characterized using a receiver over the frequency domain using MIL-STD 461 RE102 and RE103, but the POI of a pulsed emission event at each frequency is either low or the time duration for the test scans is long. Limited insight be drawn regarding the non-stationary phenomena captured in these scans. While the time duration of capture in the spectrum analyzer is higher, an oscilloscope with both sufficient sampling rate (above the Nyquist frequency) and memory can still ensure a high POI in the time domain for certain thrusters. In this paper a new technique is presented for analyzing time domain radiated emissions from electric propulsion thrusters. By using a high-speed oscilloscope sampling above the Nyquist frequency and taking advantage of digital filtering, we can not only scan the frequency space over the time domain to identify and characterize pulsed emissions, but also retain high frequency resolution.

Digital filtering offers an effective approach for performing frequency separation and time domain signal restoration, and allows the user to select desired filter characteristics and bandwidth in the post-processing phase. This type of time-frequency analysis can be useful for, 1) practical purposes, such as for companies who want to perform a highly versatile time domain analysis with minimal testing, and 2) scientific purposes, such as for researchers interested in studying the dynamics of thrusters. In this paper, we take an example of a time domain radiated emission measurement from Aerospace's GPT-1 electric thruster using an oscilloscope and investigate the use of digital filtering to reproduce spectral and temporal scans, such as is traditionally done with "LSCX" and "Zero Span" measurements. Then, we selectively apply the digital filter to create different frequency passband characteristics. The technique is developed direclty from data analyzed using previous techniques to study pulsed emission in the literature.[3,4]

II. Thruster Radiated Emission Characteristics

For the purpose of this study, Aerospace's GPT-1 thruster is used - the details of the data used here are described in Beiting et. al.,[4] and the corresponding characteristics of the thruster operating in the S-band ("Ch3") are shown in Figures 1a and 1b. For this measurement a double ridge horn antenna was connected to a 2-4 GHz bandpass filter and passed through a low noise amplifier - attenuator - low noise amplifier configuration. A 15 GHz bandwidth oscilloscope (Tektronix TDS6154C) is used to capture data record lengths of 8 x 10^6 samples at 50 picoseconds per point for a record length of 400 microseconds. Antenna factors, AF, and gains and losses, C, are measured and used to calculate the electric field at the antenna 1 m away from the source, $E(V/m) = V * AF/C$. By focusing on one narrow frequency band at a time, the AF and C terms are able to be assumed to be constant as function of frequency. To calculate the electric field over a broadband, the correction terms AF and C need to be applied in narrow frequency band sections until the broadband can be pieced back together. The emissions behavior above 1 GHz for this thruster tends to be quasi-periodic in 100-200 microseconds intervals, consistent with Beiting et. al.'s observations.[3] Moreover, the pulses are approximately 0.1 to 5 microseconds in duration, and for pulses of 100 nanoseconds duration, the spectral bandwidth has been shown to be approximately 5 MHz. Using this information, we can focus our attention to Pulse 2 shown in Figure 1 to develop an appropriate digital filter to understand the evolution of this frequency over time.

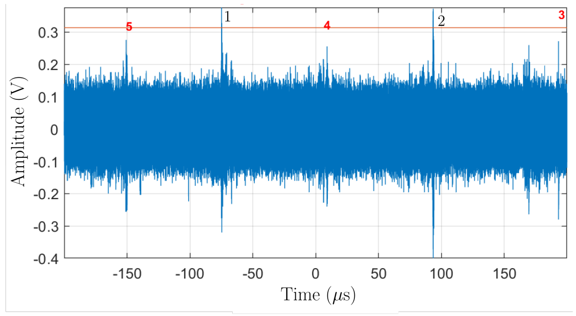

(a) Figure 1a: Time domain radiated emissions from GPT-1 recorded on 15 GHz bandwidth oscilloscope with 20 GS/sec from 2-4 GHz.

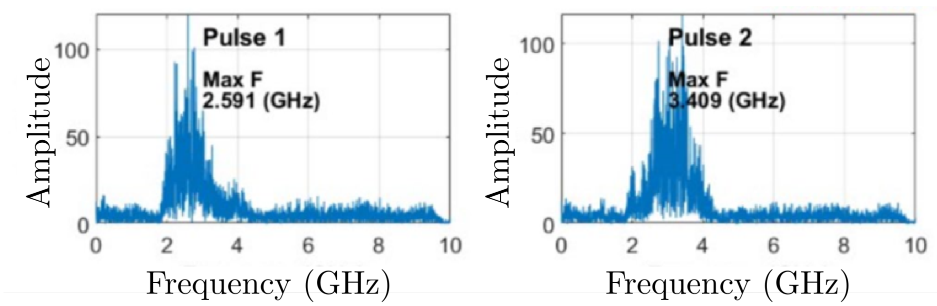

(b) Figure 1b: Frequency domain around pulses derived from time domain data. This study focuses on Pulse 2, labeled in Figure 1a in the time domain by a black "2".

Figure 1. Representative radiative emissions from Hall thruster characterized from time domain data.

III. Digital Filtering Concept

Often radiated emission experiments are a trade-off between time and frequency domain resolutions. Zero span time domain measurements are meant to monitor a given narrow frequency band over an extended period of time, whereas the LSCX time domain measurements are broadband over a short period of time. Satellite users are typically concerned with specific frequencies that match their specific system, and it can be difficult to predict future use of a thruster during EMI qualification testing. Therefore, there is a need to be able to "sift" through the frequency domain to monitor specific frequencies over time, and this is precisely what digital filtering can provide.

The general concept is illustrated in Figure 2. A broadband time domain signal consisting of two tones at 100 and 50 Hz at 1 and 2 volts amplitude, respectively, are captured and sampled above the Nyquist frequency at 1000 samples/second, see Figure 2a. Note in this two tone signal that the 50 Hz signal is abruptly shut-off at halfway through the time segment. The signal is then decomposed into the frequency domain utilizing a Discrete Fast Fourier Transform (DFFT), shown in Figure 2b. Spectral leakage in the form of a sinc function is observed in the time frequency domain around the 50 Hz signal due to the 50 Hz signal turning off abruptly at 0.5 μs. It is important to note that a single Fourier transform over the 2 V amplitude of the 50 Hz signal in the frequency domain is represented as 1 V instead of 2 V due to the effect of averaging the amplitude at 50 Hz over the entire 1 second window. This will be discussed more later. The Inverse Discrete Fourier Transform (I^{-1}-DFT) is is used to successfully recover the original time domain signal from the frequency domain in Figure 2c. An idealized passband is implemented digitally using a "brick-wall filter"[5,6] at time zero as shown in Figure 2d, isolating only the band of interest, shown in Figure 2e. The final, narrowband signal of interest is then reconstructed using the I^{-1}-DFT in Figure 2f from the modified frequency domain data, and is shown compared to Figure 2c which had no filtering. The 2 V 50 Hz tone is successfully captured with the digital filter and the 1 V 100 Hz tone is successfully removed. Since the filter removed the side lobes of the sinc function around the 50 Hz tone, we also see the noise this introduces when recovering the time domain with the I^{-1}-DFT in 2f.

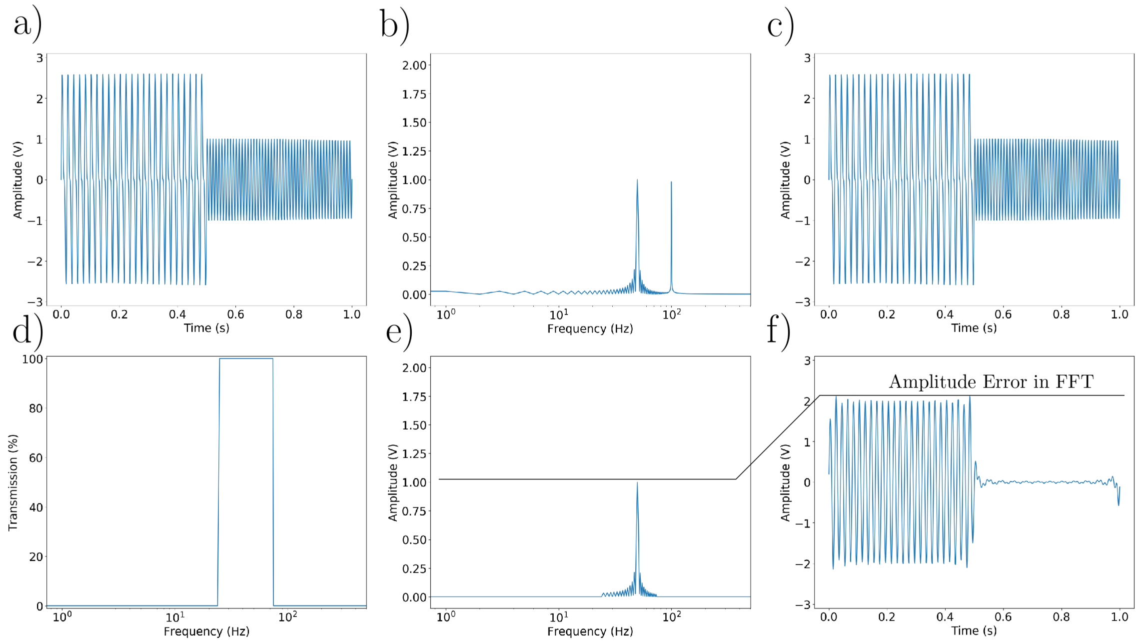

Figure 2. a) Original signal, b) after applying DFFT, c) recovering original signal using the I-DFT^{-1}, d) visualizing filter characteristics, e) frequency domain after filtering at time zero, and f) recovering time domain from filtered data. Note inputs signals are: 2 V, 50 Hz, 50% duty cycle, and 1 V, 100 Hz, 100% duty cycle.

We wish to investigate the use of digital filters to scan both the frequency and time domains within the thurster data set chosen. As an example, we have chosen to inspect Pulse 2 as shown in Figure 1 for further investigation. First, we focus on being able to scan the frequency over time, and to do this, we must consider the trade-off between the record length and bandwidth according to:

$$\Delta f\,(Hz) = \frac{sample\,rate\,(sam/sec)}{\#\,of\ samples} \tag{1}$$

Using Equation 1 we can construct Figure 3, where we have summarized the trade-space with respect to varying filter parameters around the frequency of interest. We note that the sample rate is fixed by the oscilloscope settings, whereas the number of samples is set by the selected dwell time, or window length, in post-processing ($sample\,rate * dwell\,time$). As the dwell time increases, the temporal resolution of the Fast Fourier Transform (FFT) is reduced and the frequency resolution is increased. The bandwidth has to be sufficient to be able to capture the signal of interest. In the limit, the entire record length of 400 μs can be processed for the highest frequency resolution and lowest time resolution. For a 10 μs dwell time (i.e., the temporal resolution) with 10 MHz bandwidth using 20 GS/sec, we have windows composed of 200,000 samples with a frequency resolution of 100 kHz. In a practical scenario, the bandwidth of the filter would be selected to model the bandwidth of a particular satellite transceiver system; in this study, a bandwidth of 10 MHz is selected to ensure the entire pulse bandwidth is captured inside the filter. A boxcar window function, of which the rectangular function is a special case, is defined for simplicity:

$$W(\Omega) = \begin{cases} 1 & \text{if } (f_c - f_{BW}) \leq f_c \leq (f_c + f_{BW}), \\ 0 & \text{otherwise} \end{cases} \tag{2}$$

The center frequency of the band is chosen to match the peak frequency of Pulse 2 in Figure 1, which is 3.409 GHz. Thus, using Equation 2, and Figure 3, we can construct a digital filter that will maintain sufficient temporal and frequency resolution for non-stationary events in the thruster with 10 μs dwell time and 10 MHz bandwidth.

In Figure 4, a bandpass filter of 10 MHz using 10 μs windows around Pulse 1 and Pulse 2 is constructed around the center frequency of 3.409 GHz, which is designed to capture only Pulse 2. In Figure 4a, Pulse

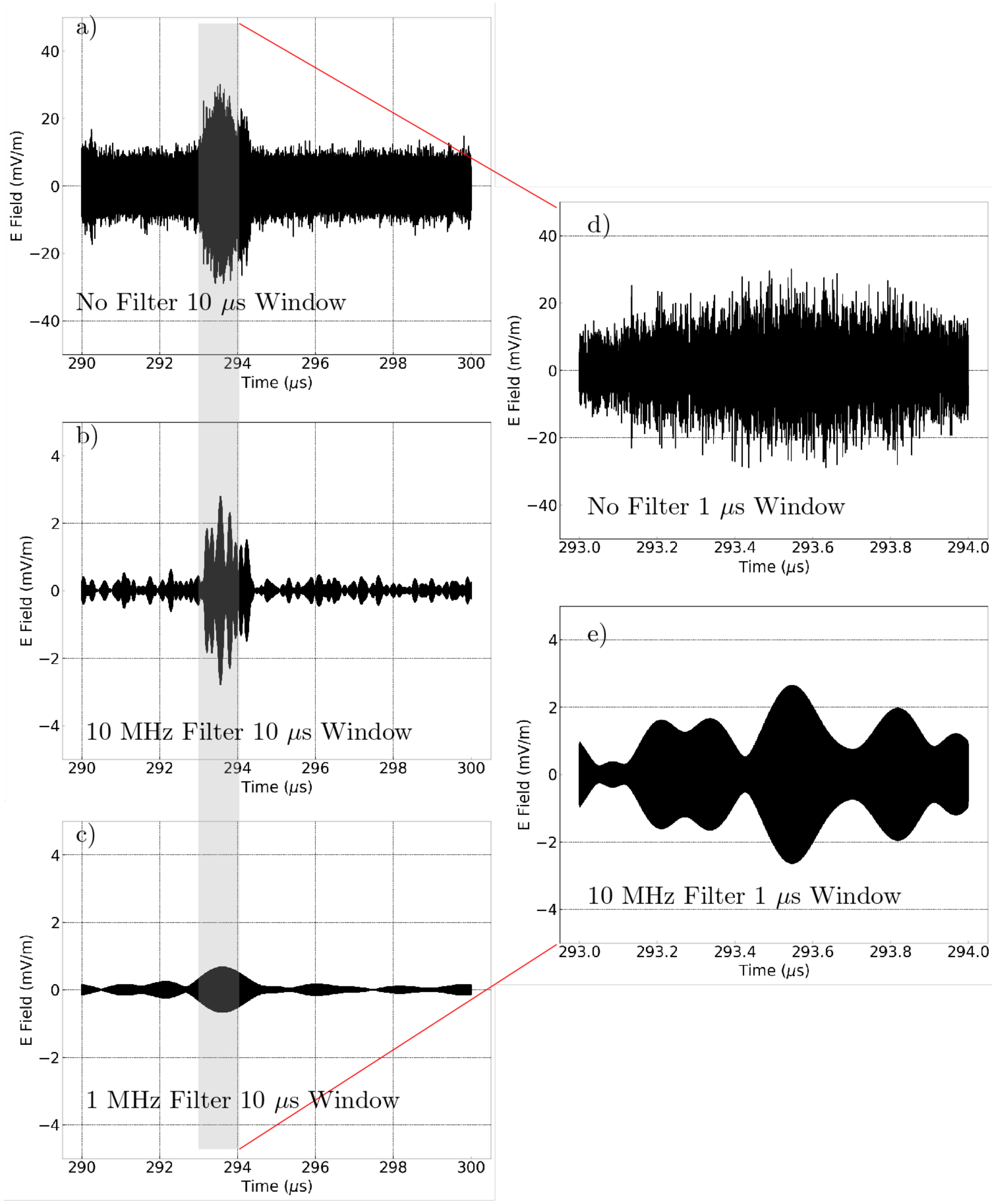

Figure 3. a) 10 μs window around Pulse 2 extracted from Figure 1a, b) 10 MHz filter in 10 μs window around 3.409 GHz capturing Pulse 2, c) 1 MHz filter in 10 μs window around 3.409 GHz does not capture full bandwidth of Pulse 2, d) 1 μs window around Pulse 2 extracted from Figure 3a shown in the gray bar, and e) 10 MHz filter in 1 μs window around 3.409 GHz shows reduced slightly reduced peak amplitudes with reduced frequency resolution.

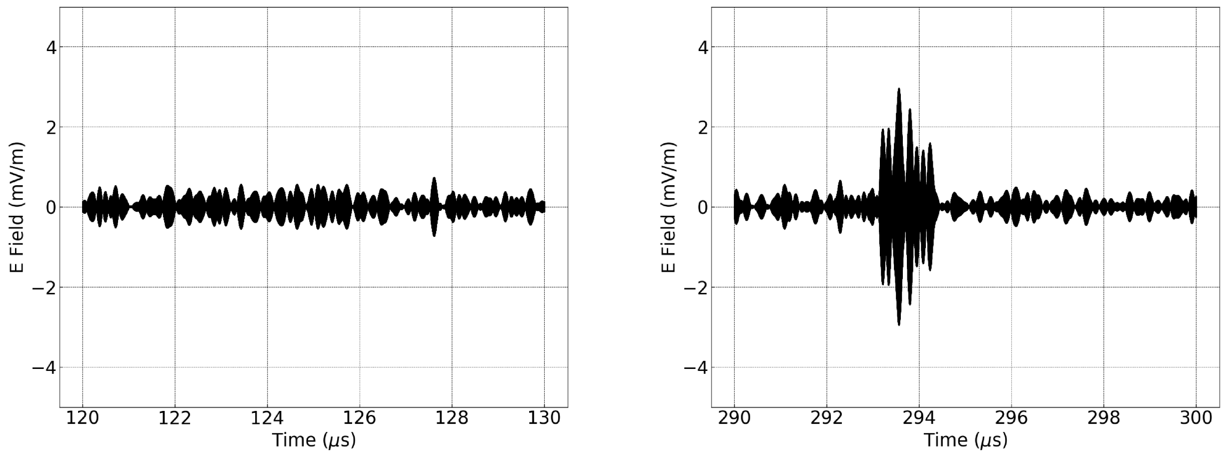

(a) Figure 4a: Pulse 1 at 2.591 GHz filtered out by 10 MHz bandpass filter.

(b) Figure 4b: Pulse 2 at 3.409 GHz captured using digital bandpass filter.

Figure 4. Using digital filter with 10 MHz bandwidth around 3.409 GHz and 10 μs windows to capture pulse information.

1 at -75 μs at 2.591 GHz is filtered out, and at +95 μs, Pulse 2 at 3.409 GHz is successfully captured; this verifies the filter functions as expected.

Typical time domain measurements performed using a spectrum analyzer can be reproduced using the broadband oscilloscope data by applying the desired digital filter to the dataset. Digital filters are flexible by design, and can be used to readily capture peak signals inside each window; this information can then be used to perform a BER statistical analysis.[7] A 10 MHz filter centered around 3.409 GHz is constructed by piecing together 40 windows of 10 μs in a sequential fashion until the entire 400 μs trace is reconstituted as shown in Figure 5a. Note that for simplicity no overlapping of windows is used for simplicity purposes, but that this may improve the fidelity of the time domain signal reconstruction. Using Figure 5a, we are able to construct zero span and associated histogram plots for assessing BER, see Figures 5b and 5c, respectively. Depending on the required time-frequency resolution, there exists a trade-space for dwell time and the number of samples for building a statistical analysis.

In addition to monitoring frequencies of interest over time, we are also able to construct similar peak hold measurements typically performed using receivers and standardized measurement techniques described in MIL-STD461. To do so, we have implemented 10 MHz bandwidth filters over the entire frequency space of interest to construct the peak amplitudes at each frequency from all 40 of the 10 μs dwells (windows) inside the 400 μs trace. We are readily able to capture not only the transient peaks with a higher POI, but also potentially do so in significantly less time than would be required for standardized testing. The analysis presented here does not replace standardized testing, it could be a useful technique for pre-qualification and characterization. The results are shown in Figure 6.

IV. Transient Capture

The purpose of radiated emissions testing is to capture and characterize the peak radiated emissions from thrusters. The tool most common for doing this is the DFFT via the FFT algorithm:

$$X[n] = \sum_{n=0}^{N-1} x[n] \cdot e^{\frac{i2\pi}{N} kn} \tag{3}$$

where X_n is the Fourier transform of the signal x_n. However, there are two things to consider while employing the Fourier transform. First, it has an intrinsic coupling and inverse relationship between frequency and time resolution. As the frequency resolution increases, the time resolution decreases. Thus, at high frequencies, the true amplitude of transient emissions can be missed due to either averaging the FFT over a timescale that exceeds the pulsed emissions, or due to filter artifacts when recovering the time domain via

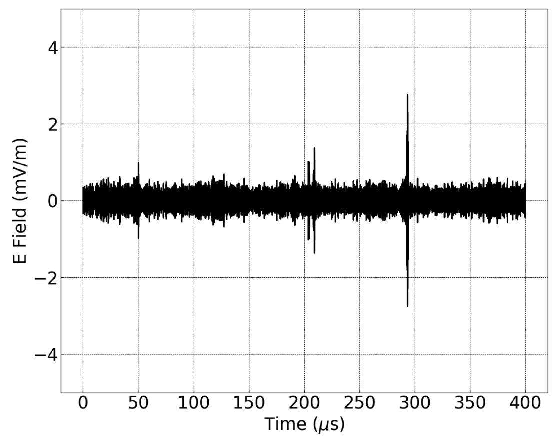

(a) Figure 5a: Time domain around 3.409 GHz reconstructed through digital filter with 10 MHz bandwidth using 10 μs windows.

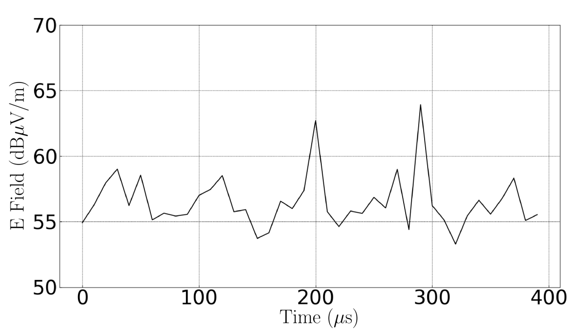

(b) Figure 5b: Zero span type measurement reconstructed from peak inside each 10 μs window.

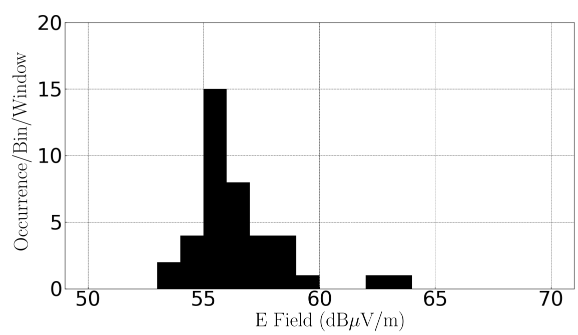

(c) Figure 5c: Statistical analysis can be performed using peak values from zero span data swhon in Figure 5b.

Figure 5. Zero span trace can be reconstructed, and from this a statistical analysis can be performed. The number of points is controlled by the dwell time in each window.

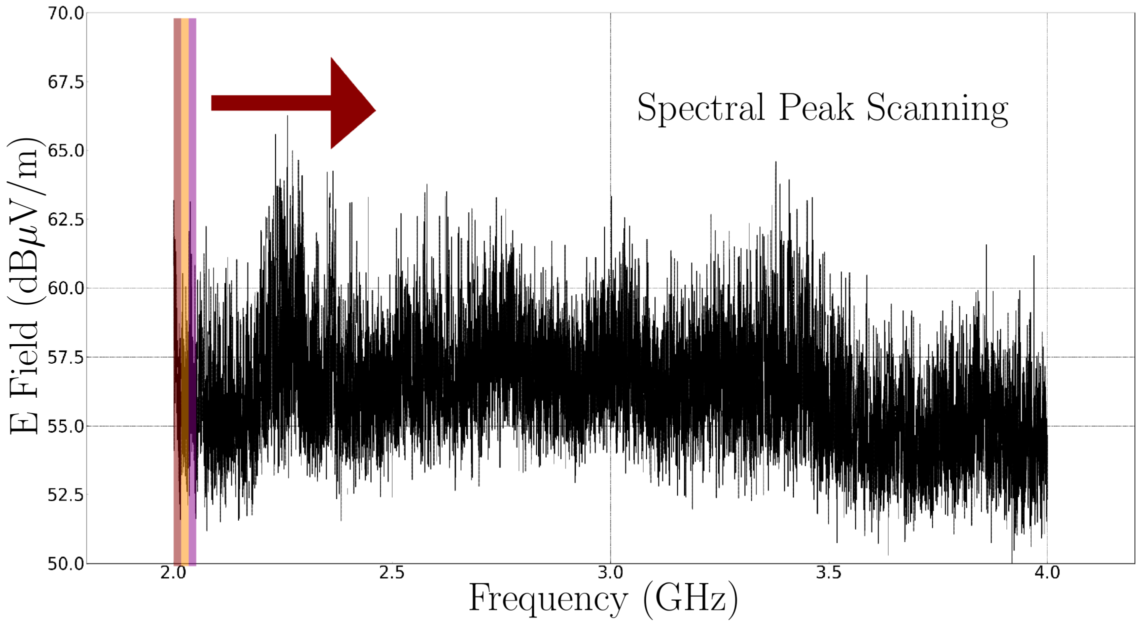

Figure 6. Spectral "peak hold" scan for a 400 μs dwell with maximum transient capture time of 10 μs. A 10 MHz digital bandpass filter with 10 μs windows is applied over the entire frequency and time domain, correcting for the frequency dependent antenna factor, gains, and losses as constants in each step (band).

the I^{-1}-DFT, as was shown in Figure 2e. Second, since thruster emissions has been shown to exhibit non-stationary behavior, particularly above 1 GHz. For this reason, the Short-Time Fourier Transform (STFT) can be employed that incorporates the Fourier transform with a window function:

$$STFT\{x[n]\}(m,\omega) \equiv X(m,\omega) = \sum_{n=-\infty}^{\infty} x[n]w[n-m]e^{-i\omega n} \tag{4}$$

where $X(m,\omega)$ is the STFT of signal $x[n]$, and $w[n-m]$ is the window function. To compensate for the use of this window function, overlap in the time domain of consecutive FFTs is done to ensure high fidelity of the amplitude response recorded in the frequency domain representation. This approach forms the mathematical underpinning of Real-Time Spectrum Analysis (RTSA). The concept of POI considers both the instrument time off between measurements and the fastest transient signal a measurement can capture, and is important when creating a spectrogram to display the results of the STFT. By restricting ourselves to post-processing, we are not limited by the speed of FFT processors in a given instrument, but instead only by the sample rate of the oscilloscope. The benefit of RTSA is to be able to capture not only frequency hopping signals while taking a measurement, but also any transient dynamics. Thus, we can relax the desire to capture these frequency hopping signals during testing in favor of being sure to capture all the transient signals of interest using broadband data and post-processing. Unless the RTSA has the ability to measure transient events down to 100 ns with 100% POI, there is a distinct likelihood that even a RTSA unit is missing content from the physical events inside the thruster. We can readily employ sufficient overlap as needed to ensure high fidelity construction of the frequency content over time. For a 100% POI, with 99% overlap, the minimum transient time event that can be recorded is given by:

$$T_{min} = \frac{N\,(number\,of\,samples)}{sample\,rate} \tag{5}$$

where N is determined by $N = (window\,size) + (time\,record\,length) - 1) - P$, and P is the number of overlap points. For a 99% overlap at 10 μs, this translates to a minimum transient event capture time of approximately 10 μs. The results are shown in Figure 7, and we can make out the five different coherent pulse events as fairly broadband vertical yellow bars on top of the blue incoherent noise present during thruster operation.

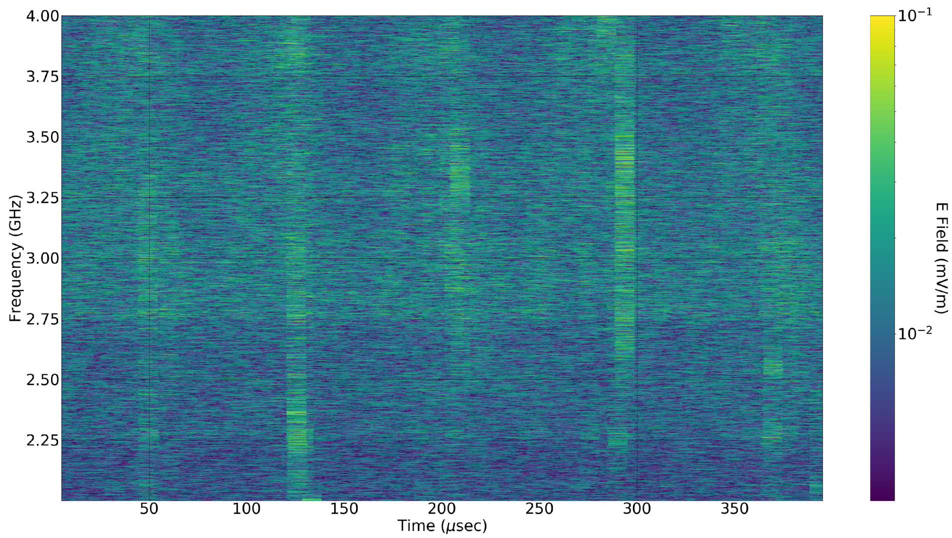

Figure 7. Spectrogram of S-band constructed from the oscilloscope data shown in Figure 1a and corrected to an electric field, plotted in log-scale. The pulses identified from Figure 1 are clearly seen in the spectrogram. The color map is plotted in log-scale. Each line across the x-axis is a zero span trace. Note that Figure 6 represents the peak amplitude extracted from across the x-axis of the spectrogram for each frequency.

For 100 ns events like those expected in this thruster, we would need to use 0.1 μs dwells, but this would leave us with insufficient frequency resolution of 10 MHz. Whereas the optimized STFT is limited by the trade-off between frequency and time resolution, for highly non-stationary peak signals, we can use the Continuous Wavelet Transform (CWT):

$$Wf(u,s) = \int_{-\infty}^{+\infty} f(t)\frac{1}{\sqrt{s}}\Psi^{*}(\frac{t-u}{s})dt \tag{6}$$

where u is the time and s is the scale. The CWT calculates the convolution between the wavelet function chosen and the input signal. A wavelet is a function Ψ that is translated by u and scaled by s, and ultimately allows time resolution to dilate at lower frequencies and compress at higher frequencies[8] as desired for different sections of the input signal - the details of the discrete implementation of the CWT are described in Mallat et. al. For the purpose of this study, both real-valued and complex Morlet wavelets are used to monitor Pulse 2. In Figure 8 we are able to zoom and center around 294 μs with a window of ± 10 μs inside of Pulse 2 to observe the time evolution of all frequencies. For this study, we defined 10 "voices" and 8 "octaves" scaling on a Morlet wavelet to provide at least 10 different sized frequency bands in the 2-4 GHz S-band shown which evolve over the 400 μs time period. This scaling approach is chosen for convenience and is equivalent to defining a scale by $a_0 = 2^{\frac{k}{number\,of\,voices}}/(sample\,rate)$, for k integers between number of voices and the number of voices times the number of octaves. The frequency bands are then recovered by dividing the center frequency of the wavelet (0.8125) by this scaling to recover the corresponding frequency ranges, and the resulting frequency resolution varies approximately from 150 to 250 MHz across the S-band. For the first time, we have attempted to use wavelets to achieve higher temporal resolution than that which is afforded by STFT to elucidate the true time period of the pulsed emission from the thruster. Interestingly, we observe that the pulse is broadband and that longer lasting in some frequency domains than others; between roughly 2 μs from 3.25 to 3.50 GHz to less than 1 μs from 2.25 to 2.50 GHz. Thus, wavelet analysis and digital techniques allow the user to probe not only the anticipated impact on communication systems due to thruster emissions with higher fidelity, but also may provide insight into the underlying dynamics in the thruster by unveiling the timescale evolution of non-stationary phenomena in the thruster.

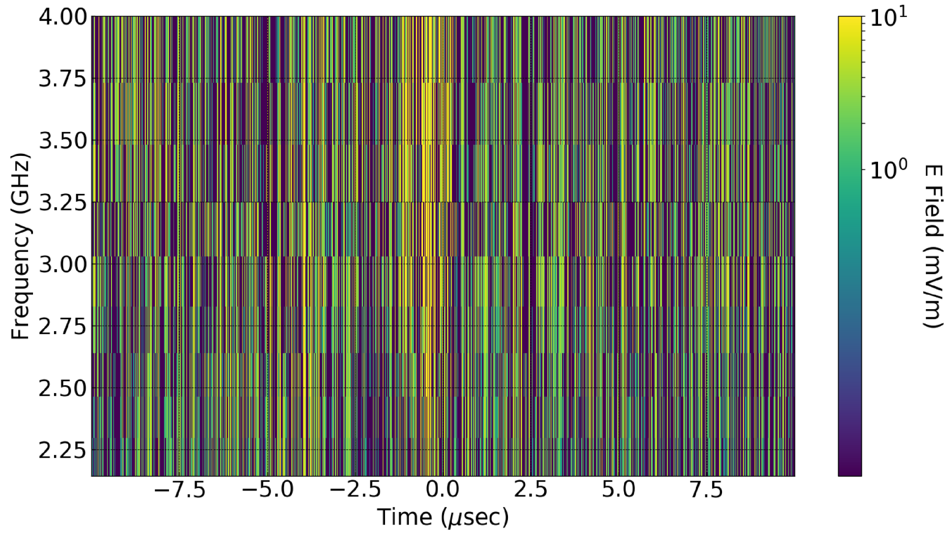

(a) Figure 8a: Scalogram showing high time resolution around 294 μs with ± 10 μs of nearby data. Pulse 2 is visible around 0 μs, and the time duration of the pulse in the corresponding broadband varies in each frequency band.

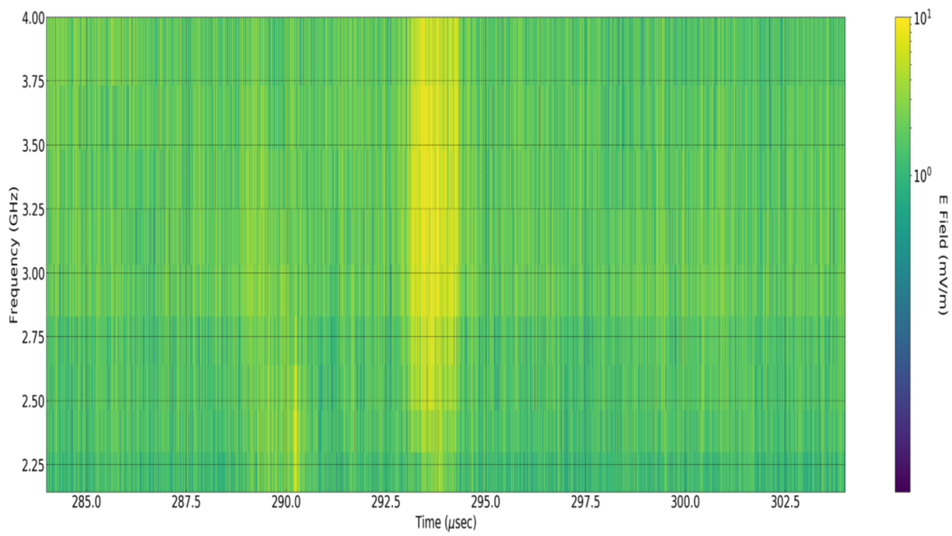

(b) Figure 8b: Using complex Morlet transform with bandwidth parameter 3 and center frequency of 1 Hz.

Figure 8. Real and complex Morlet wavelets can be used to monitor either peaks and discontinuities, or amplitude and phase, respectively. The complex wavelet has smoothing in the x- and y-axes attributed to the non-zero bandwidth parameter, which results in a loss in time resolution and recovers a signal similar to the spectrogram. Amplitude fluctuations inside each band of Pulse 2 can be visualized over time.

V. Discussion & Conclusion

In our previous experiments, broadband time domain radiated emission data has been collected for two reasons. First, we used a crystal diode to slow down the radiated emissions and be able to capture significant trace length for statistical analysis. Second, we used the maximum sampling rate to capture the frequency content from the thruster radiated emissions. In this paper, we have taken the utility of this high sampling rate data set to the next level. We have established the ability to implement digital filters with the appropriate frequency adaptive corrections to construct 1) narrowband time domain data, 2) zero span time domain data, 3) BER statistical analysis for an oscilloscope trace, 4) spectrogram monitoring capability, and 5) spectral peak amplitude monitoring over the broadband.

There are three different ways to perform time-frequency analysis; Fourier transforms, Short-Time Fourier Transforms, and Continuous Wavelet Transforms. First, the Fourier transform can be employed over a specified time domain. This approach has been used to study the spectral content of pulses in radiated emissions from thrusters in the past. However, this method is an average of the spectral content within the dwell time of the FFT, which can lose both amplitude and temporal information for certain non-stationary signals such as those found in Hall thrusters. Second, using STFTs, we can reconstruct the temporal features of the frequency evolution by carefully employing overlap between windowed time domains. This approach has an intrinsic trade-off between time and frequency resolution, but allows for the ability to capture a degree of intermittent, non-stationary signals. However, to favorably manipulate the inverse relationship between time and frequency resolution, we can use wavelets to be able to achieve high temporal resolution at high frequencies (and low temporal resolution at low frequencies). Wavelet analysis allows the ability to capture non-stationary behavior closer to the observed scale of temporal evolution of plasma dynamics in the thruster; for example, looking at Figure 1, we can see that there were at least 5 pulses in 400 μs time frame, and that these pulses occurred at different frequencies according to the Fourier transform. With insufficient temporal resolution, it is possible that the true localization of the pulse in the window is not known, and also that the true peak amplitude is not being properly captured due to averaging over a dwell time that exceeds the pulse event time. Since each pulse peak amplitude in frequency domain vary across the 400 μs trace analyzed, the GPT-1 thruster radiated emissions in the S-band may possess a frequency hopping behavior; in other words, the frequency is a function of time. Moreover, it is important to note that there may also oscilloscope driven artifacts in the analyzed data such as spurs and interleaving effects to consider, but these are beyond the scope of this study.

While these tools developed are not a replacement for standardized testing, future work will 1) scientifically, expand on the use of wavelets for studying the physics and non-stationary phenomena associated with thruster radiated emissions, and 2) practically, we will compare the results here with standardized measurements to understand the limitations of using digital signal processing for characterizing thruster radiated emissions performance. The tools developed here for oscilloscope traces are to be considered characterization tools only, and they may benefit former customers who have time domain radiated emission data, as well as future customers who desire to obtain more information with less available resources.

Acknowledgments

This work was supported by The Aerospace Corporation's Sustained Experimentation and Research for Program Applications. The authors would like to acknowledge Edward Beiting, Michael Rolenz, and Taylor Matlock for their support and mentorship.

References

[1]M. Dulligan, R. Bromaghim, J. Zimmerman, R. Salasovich, D. Hardesty, and L. Johnson, "Effect of ESEX 26-kW Arcjet Operation on Spacecraft Communications," *Journal of Propulsion and Power*, vol. 18, no. 4, pp. 754–762, 2002.

[2]W. Hreha, R. Singh, S.-L. Liang, D. Burr, and M. Day, "SPT Interference Assessment in Communication Satellites," in *22nd AIAA International Communications Satellite Systems Conference & Exhibit 2004 (ICSSC)*, p. 3216, 2004.

[3]E. J. Beiting, R. Spektor, and X. L. Eapen, "Parameters Influencing the Generation of the L , S , and C-bands (1 – 8 GHz) Emission from Hall Thrusters," in *31th International Electric Propulsion Conference, 20-24 September 2009, IEPC-2009-072, University of Michigan, USA*, pp. 1–9, 2009.

[4]E. J. Beiting, R. Spektor, and X. L. Eapen, "Time-Domain Characteristics of 0.5-8 GHz Pulsed Emission from Hall Thrusters," in *46th AIAA/ASME/SAE/ASEE Joint Propulsion Conference & Exhibit, 25-28 July 2010, AIAA 2010-6777, Nashville, TN*, p. 6777, 2010.

[5]P. A. Lynn and W. Fuerst, *Introductory Digital Signal Processing with Computer Applications.* John Wiley & Sons, 1998.

[6]S. W. Smith, "The scientist and engineer's guide to digital signal processing," 1997.

[7]E. J. Beiting, X. L. Eapen, J. E. Pollard, M. Gambon, F. R. Marchandise, and M. Oberg, "Electromagnetic Emissions from PPS® 1350 Hall Thruster," in *31th International Electric Propulsion Conference, 20-24 September 2009, IEPC-2009-071, University of Michigan, USA*, 2009.

[8]S. Mallat, *A Wavelet Tour of Signal Processing.* Elsevier, 1999.